Journal of Computational Applied Mechanics 2025, 56(1): 15-42
DOI: 10.22059/jcamech.2024.383880.1256

RESEARCH PAPER

Forced vibration control of Timoshenko's micro sandwich beam with CNT/GPL/CNR reinforced composites integrated by piezoelectric on Kerr's elastic foundation using MCST

Mohammadjavad Jafari [a], Mehdi Mohammadimehr [b,*]

[a] *PhD Student, Department of Solid Mechanics, Faculty of Mechanical Engineering, University of Kashan, Ghotb Ravandi Blvd., Kashan, Iran*

[b] *Professor Department of Solid Mechanics, Faculty of Mechanical Engineering, University of Kashan, Ghotb Ravandi Blvd., Kashan, Iran*

Abstract

In the present article, forced vibration control of Timoshenko's micro sandwich beam based on modified couple stress theory (MCST) is studied. The face sheets are made of three-phase reinforced nanocomposite including resin, piezoelectric and CNT\CNR\GPL materials, and top and bottom layers operate as actuator and sensor, respectively. The micro sandwich beam is placed on Kerr's foundation and subject to harmonic force with resonance excitation frequency. By considering the equations of motion in the state-space form and using LQR, the amplitude of forced vibrations of the micro beam is optimized. Furthermore, the effects of various parameters including the volume fraction of CNT, GPL and CNR, three parameters of Kerr's elastic foundation and three natural frequency modes on the suppression and settling time and forced vibration response of a micro sandwich beam is investigated. In this research, for various types and volume fractions of nanocomposites, the second and third natural frequency modes increase 3.5 and 6.7 times, respectively, compared to first natural frequency mode. Also, the Kerr foundation increases the first, second and third mode of natural frequency by about 46%, 13.1% and 7.7%, respectively.

Keywords: Vibration control; Micro sandwich Timoshenko beam; MCST; LQR; Various nanocomposites; Kerr's elastic foundation; Integrated by piezoelectric;

1. Introduction

In many industries that require light and high-strength components, such as automotive, marine, aerospace, shipbuilding, transportation, electronics, biomedical engineering, nuclear engineering, the use of sandwich structures has expanded greatly. To increase the characteristics such as strength, aspect ratio, stiffness and improve the performance of sandwich structures, they are reinforced with nanoparticles. Usually, in the face sheet layers of sandwich structures, these nanoparticles are added to the matrix in the composite structure and lead to the increase in the modulus of elasticity and yield strength. One of the most widely used nanoparticles is carbon nanostructures such as carbon nanotubes (CNTs) [1] , graphene platelets (GPLs) [2-4] and carbon nanorods (CNRs) [5-7], which can improve the functional characteristics of composites and sandwich structures as reinforcements. In the literatures, the researchers is investigated buckling [8, 9], bending [10], impact response and vibration analysis [11, 12] of the carbon nanostructures and various parameters on sandwich structure. Also, by adding other materials such as piezoelectric materials that react to electric and magnetic

* Corresponding author. Tel.: +98-31-55913432;

E-mail address: mmohammadimehr@kashanu.ac.ir

fields and converting this type of composite to three-phase composites, sandwich structures become smart structures.

Vibration is one of the problems that engineers always face and it causes disruption in the performance of the structure, so finding a suitable method to control vibrations is always of great importance [13]. So far, three methods to control vibrations including active control [14], semi-active control [15] and passive control [16, 17] are used. One of the vibration control methods is the active vibration control method, which is widely used. To control the vibrating structure, the use of piezoelectric materials as sensors and actuators has been proposed [18-20]. The piezoelectric material can be used as a thin layer patched on the structure [21, 22] or as a separate layer of the sandwich structure [23, 24] or as a three-phase composite. One of the applications of active vibration control is in the aerospace industry, such as the vibration control of solar arrays, where the solar array is considered as a flexible cantilever thin plate with composite macro fiber (MFC) piezoelectric patches and the Proportional-Integral-Derivative (PID) method is used to suppress vibration [25]. Also, for lightweight thin-walled structures on spacecraft, which are considered as Euler-Bernoulli beam with piezoelectric patches under fixed harmonic excitation and variable harmonic excitation, active vibration control method and vibration suppression algorithm is considered [26]. Active vibration control is also effective on aircraft wings that are considered as integrated composite sandwich plates (ICSPs) embedded macro-fiber composites (MFC) based on the first-order shear deformation theory (FSDT) with incompletely constrained boundaries and irregular geometric shapes with piezoelectric effect [27]. Another application of active vibration control in the aerospace industry, the solar wing as a vital energy component of spacecraft, often faces challenges due to vibrations and deformations during the orbit, which affect the pointing accuracy of the spacecraft and operational performance, a new method Actuation based on an embedded piezoelectric actuator (EPA) is proposed [28]. For a fixed-free cantilever composite beam equipped with piezoelectric materials where the sensors and actuators are bonded to the upper and lower surfaces at arbitrary locations along the beam's length. Numerical analysis is showed that the closer the actuator patches are to the end of the clamped, the settling time is shorter. As a result, the longest settling time occurs at the free end and the least at the clamped of cantilever beams [29]. In active vibration control, the feedback gain coefficient affects the reduction of the structure's oscillation amplitude and the natural frequency, and by adjusting the feedback gain coefficient, the vibration of the structure can be significantly reduced [30-33].

In vibration control, the use of a suitable algorithm is very effective to improve the performance of the control system and the voltage piezoelectric layer plays an important role in this field. For multi-layer sandwich composite piezoelectric micro-beams is suggest that the Linear Quadratic Integral (LQI) control scheme [34]. One of the linear controllers is based on solving the Riccati algebraic equation and is very suitable for linear vibrations. In these controllers, state feedback is considered based on linear quadratic regulator (LQR) [35, 36]. Other control algorithm is filtered-x least mean square (FxLMS) algorithm, which is used for an analysis model of adaptive active vibration control system of composite laminated plate using macro fiber composite (MFC) piezoelectric patches [37]. Also, feedback control based on the integral force feedback (IFF) algorithm is considered for active vibration control of a multiple degrees of freedom (multi-DOFs) strategy based on a piezoelectric platform [38].

Beams have a wide range of applications, from giant structures such as spacecraft, ships, and submarines to micro-electro-mechanical systems (MEMS) and nano-electro-mechanical systems (NEMS), including micro actuators, micro sensors [39] and biomedical applications.

Usually, the large amplitude vibrations associated with the nonlinear system are controlled using linear controllers such as positive position feedback (PPF). In an experimental approach for a clamped composite beam, a PPF controller with single-input single-output (SISO) architecture and multiple-input multiple-output (MIMO) architecture is developed [40, 41].

By reviewing the literature, it was found that the active control of forced vibrations in the resonant frequency range of sandwich micro beams with nanocomposite layers has not been considered. Also, there is no discussion about sandwich micro beams with nanocomposite layers on elastic foundation and the effect of different nanocomposites and also various parameters of elastic foundation on the active control of forced vibrations. Therefore, the control of forced vibrations of a Timoshenko sandwich micro beam with different face sheet (CNT, CNR and GPL) on the Kerr's elastic foundation, which is subjected to the harmonic force with the resonance excitation frequency, is investigated. The forced vibration and deflection responses are analyzed for the various volume fraction CNT, GPL and CNR. The settling time, the amplitude of deflection and first natural frequency mode for the constant volume fraction of the three nanocomposites (CNT, GPL and CNR) are compared. The effects of various volume fraction and various nanocomposite on three modes of natural frequency are investigated. Active vibration control for three types of elastic foundations including Winkler, Pasternak, and Kerr is also discussed. Also, the effects of various foundations on increase or decrease of first, second and third natural frequency are discussed. Finally, the force vibration response and settling time of Timoshenko's micro sandwich beam with CNR reinforced integrated by piezoelectric on Kerr foundation is analyzed for three modes of natural frequency. Due to the dimensions of the micro beam, governing equations are derived based on modified couple stress theory that it consider small-scale effect. To solve the equations of motion, the state space form has been used, which leads to reducing the order of the equations. In the control algorithm, state feedback is considered based on linear quadratic regulator (LQR).

2. Mechanical properties

In this research, the three-phase reinforced nanocomposite face sheets are made of piezoelectric material (PVDF) as fiber reinforced by CNT or CNR or GPL in the epoxy matrix. Thus, the material properties of the resin\CNT are estimated by Halphin-Tsai semi-empirical equations as follows [42]:

$$E_m^{CNT} = \left(\frac{3}{8}\left(1 + 2\frac{l_{CNT}\eta_L V_{CNT}}{d_{CNT}(1-\eta_L V_{CNT})}\right) + \frac{5}{8}\left(\frac{1+2\eta_d V_{CNT}}{d_{CNT}(1-\eta_d V_{CNT})}\right)\right)E_{resin} \tag{1}$$

$$\eta_L = \frac{\left(E_{CNT}/E_{resin}\right) - \left(d_{CNT}/4t\right)}{\left(E_{CNT}/E_{resin}\right) + \left(l_{CNT}/2t\right)} \tag{2}$$

$$\eta_d = \frac{\left(E_{CNT}/E_{resin}\right) - \left(d_{CNT}/4t\right)}{\left(E_{CNT}/E_{resin}\right) + \left(d_{CNT}/2t\right)} \tag{3}$$

$$\nu_{12}^m = \nu_{resin} \tag{4}$$

$$\rho_m^{CNT} = \rho_{CNT}V_{CNT} + \rho_{resin}V_{resin} \tag{5}$$

$$G_m^{CNT} = \frac{E_m^{CNT}}{2(1+\nu_{12}^m)} \tag{6}$$

and material properties of the k^{th}GPL are defined as follows [43]:

$$E_m^{GPL} = \left(\frac{3}{8}\left(\frac{1+\xi_L\eta_L V_{GPL}^{(k)}}{1-\eta_L V_{GPL}^{(k)}}\right) + \frac{5}{8}\left(\frac{1+\xi_w\eta_w V_{GPL}^{(k)}}{1-\eta_w V_{GPL}^{(k)}}\right)\right)E_{resin} \tag{7}$$

$$\eta_L = \frac{\left(E_{GPL}/E_{resin}\right) - 1}{\left(E_{GPL}/E_{resin}\right) + \xi_L} \tag{8}$$

$$\eta_d = \frac{\left(E_{GPL}/E_{resin}\right) - 1}{\left(E_{GPL}/E_{resin}\right) + \xi_w} \tag{9}$$

$$\xi_L = 2\frac{L_{GPL}}{t_{GPL}} \tag{10}$$

$$\xi_w = 2\frac{w_{GPL}}{t_{GPL}} \tag{11}$$

$$\nu_{12m}^{(k)} = \nu_{GPL}V_{GPL}^{(k)} + \rho_{resin}V_{resin} \tag{12}$$

$$\rho_m^{GPL} = \rho_{GPL} V_{GPL}^{(k)} + \rho_{resin} V_{resin} \tag{13}$$

$$G_m^{GPL} = \frac{E_m^{GPL}}{2\left(1 + \nu_{12}^{(k)}\right)} \tag{14}$$

and also for CNR are determined as follows [44]:

$$E_{11m}^{CNR} = E_{11_{CNR}} V_{CNR} + E_{resin} V_{resin} \tag{15}$$

$$E_{22m}^{CNR} = \frac{1}{\frac{V_{CNR}}{E_{22_{CNR}}} + \frac{V_{resin}}{E_{resin}}} \tag{16}$$

$$\nu_m^{CNR} = \nu_{CNR} V_{CNR} + \nu_{resin} V_{resin} \tag{17}$$

$$\rho_{\mathrm{m}}^{\mathrm{CNR}} = \rho_{\mathrm{CNR}} \mathrm{V}_{CNR} + \rho_{\mathrm{resin}} \mathrm{V}_{\mathrm{resin}} \tag{18}$$

$$G_m^{CNR} = \frac{E_m^{CNR}}{2(1 + \nu_{12}^{m})} \tag{19}$$

The third phase of the reinforced nanocomposite is a fiber that is piezoelectric, so the properties of the three-phase reinforced nanocomposite materials are obtained as follows [45]:

$$E_{11} = E_{11piezo} V_{piezo} + E_{11m}^{CNT/GPL/CNR} V_m^{CNT/GPL/CNR} \tag{20}$$

$$E_{22} = \frac{1}{\frac{V_{piezo}}{E_{22piezo}} + \frac{V_m^{CNT/GPL/CNR}}{E_{22m}^{CNT/GPL/CNR}}} \tag{21}$$

$$\nu_{12} = \nu_{piezo} V_{piezo} + \nu_m^{CNT/GPL/CNR} V_m^{CNT/GPL/CNR} \tag{22}$$

$$\rho = \rho_{piezo} V_{piezo} + \rho_m^{CNT/GPL/CNR} V_m^{CNT/GPL/CNR} \tag{23}$$

$$G_{12} = \frac{1}{\frac{V_{piezo}}{G_{piezo}} + \frac{V_m^{CNT/GPL/CNR}}{G_m^{CNT/GPL/CNR}}} \tag{24}$$

3. Fundamental relations of Timoshenko beam

A Timoshenko's micro sandwich beam with length L, width b and thickness h is considered. The thickness of core, top layer and bottom layer are h_c, h_t and h_b, respectively. The schematic and geometry of Timoshenko's micro sandwich beam on Kerr's foundation with CNT/GPL/CNR layers integrated by piezoelectric as sensor and actuator at the bottom and top face sheets, respectively, are shown in Fig.1.

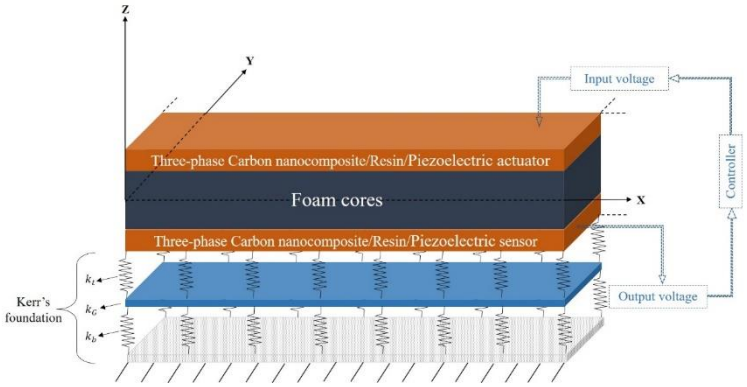

Fig.1. The schematic and geometry of micro sandwich beam on Kerr's foundation with CNT/GPL/CNR layers integrated by piezoelectric as sensor and actuator

The equations governing the sandwich structure are obtained by considering the Cartesian coordinates located in the corner of its middle plane. In this article, the displacement field of sandwich beam based on Timoshenko's beam theory is considered as follows [46, 47]:

$$\begin{aligned} u(x,z,t) &= z\psi(x,t) \\ v(x,z,t) &= 0 \\ w(x,z,t) &= w(x,t) \end{aligned} \tag{26}$$

and u, v and w are displacement components directions, respectively.

The non-zero terms of strain-displacement relations are expressed as follows:

$$\begin{aligned} \varepsilon_x &= \frac{\partial u}{\partial x} = z\psi_{,x} \\ \gamma_{xz} &= \frac{\partial u}{\partial z} + \frac{\partial w}{\partial x} = \psi + w_{,x} \end{aligned} \tag{27}$$

in which ε_x and γ_{xz} represent normal and shear stress for sandwich beams, respectively.

By considering piezoelectric material for the face sheets, the stress- strain relations of the sandwich beam for core and face sheets are written as follows:

$$\begin{aligned} \sigma_{x_{core}} &= Q_{11_{core}}\varepsilon_{x_{core}} \\ \tau_{xz_{core}} &= Q_{55_{core}}\gamma_{x_{core}} \\ \sigma_{x_i} &= Q_{11_i}\varepsilon_{x_i} - e_{31}E_z^i \qquad (i = top, bottom) \\ \tau_{xz_i} &= Q_{55_i}\gamma_{x_i} - e_{15}E_z^i \end{aligned} \tag{28}$$

where $e_{ij}, Q_{ij}, E, \varepsilon$ and σ are piezoelectric stiffness, reduced stiffness coefficients, electric field, strain and stress, respectively. Reduced stiffness coefficients are related to Young's modulus and Poisson's ratio as follows:

$$Q_{11} = \frac{E_{11}}{1 - \nu_{12}\nu_{21}} \tag{29}$$

$$Q_{55} = \frac{E_{22}}{2(1+\nu_{12})} = G_{12}$$

and also, the component electric field are defined in x and z directions as follows [48]:

$$\begin{aligned} E_z^i &= -\frac{\partial \varphi_i}{\partial z} \qquad (i = top, bottom) \\ E_x^i &= -\frac{\partial \varphi_i}{\partial x} \end{aligned} \tag{30}$$

where ϕ is the electric potential and is defined as follows (considering top and bottom layers of sandwich beam as actuator and sensor, respectively [49]:

$$\begin{aligned} \phi_{top} &= 2\frac{z}{h_t}V(x,t) + \left[z^2 - \left(\frac{h_t}{2}\right)^2\right]\varphi_{0_{top}}(x,t) \\ \phi_{bottom} &= \left[z^2 - \left(\frac{h_b}{2}\right)^2\right]\varphi_{0_{bottom}}(x,t) \end{aligned} \tag{31}$$

and also, electric displacement is explained as follows [50]:

$$\begin{aligned} D_x^i &= e_{15}\gamma_{xz}^i - \eta_{11}E_x^i \qquad (i = top, bottom) \\ D_z^i &= e_{31}\varepsilon_x^i - \eta_{33}E_z^i \end{aligned} \tag{32}$$

in which D and η_{ij} are electric displacement and dielectric coefficients, respectively.

4. Hamilton's principle

The governing equations of micro sandwich beam on Kerr's foundation under an external force are derived based on Hamilton's principle as follows:

$$\int_{t_1}^{t_2} \delta(T - U - V)dt = 0 \tag{33}$$

in which δU, δT and δV represent strain energy, kinetic energy and external work variations, respectively.

Due to the researched beam is in micro dimensions, modified couple stress theory (MCST) that consider the small scale parameter are used. Therefore, strain energy variation for core and layers of the micro sandwich beam is defined as follows:

$$\begin{aligned} \delta U &= \delta U_{top} + \delta U_{core} + \delta U_{bottom} \\ &= \int_{V_{top}} \left(\sigma_{xx}^{top}\delta\varepsilon_{xx}^{top} + \tau_{xz}^{top}\delta\gamma_{xz}^{top} - D_x^{top}\delta E_x^{top} - D_z^{top}\delta E_z^{top} + m_{ij}^{top}\delta\chi_{ij}^{top}\right) dV_{top} \\ &+ \int_{V_{core}} \left(\sigma_{xx}^{core}\delta\varepsilon_{xx}^{core} + \tau_{xz}^{core}\delta\gamma_{xz}^{core} + m_{ij}^{core}\delta\chi_{ij}^{core}\right) dV_{core} \\ &+ \int_{V_{bottom}} \left(\sigma_{xx}^{bottom}\delta\varepsilon_{xx}^{bottom} + \tau_{xz}^{bottom}\delta\gamma_{xz}^{bottom} - D_x^{bottom}\delta E_x^{bottom} - D_z^{bottom}\delta E_z^{bottom}\right. \\ &\left. + m_{ij}^{bottom}\delta\chi_{ij}^{bottom}\right) dV_{bottom} \end{aligned} \tag{34}$$

in which $\gamma_{xz}, \tau_{xz}, \varepsilon_{xx}$ and σ_{xx} are shear, normal strains and stresses, respectively.

Also, $m_{ij}$and χ_{ij} are high-order stress tensor and symmetric rotation gradient tensor, respectively, which can be obtained as follows:

$$\begin{aligned} m_{ij} &= 2Gl_2^2\chi_{ij} \\ \chi_{ij} &= \frac{1}{2}\left(\Theta_{i,j} + \Theta_{j,i}\right) \\ \Theta &= \frac{1}{2}curl(\mathrm{u}) \end{aligned} \tag{35}$$

in which Θ and u are infinitesimal rotation tensor and displacement vector, respectively. The non-zero components of χ_{ij} is state in the following form:

$$\chi_{xy} = \frac{1}{4}\left(\psi_{,x} - w_{,xx}\right) \tag{36}$$

The kinetic energy variation for core and face sheets of the micro sandwich beam is stated as:

$$\begin{aligned} \delta T = &\int_{V_{top}} \rho_{top}(\dot{u}^{top}\delta\dot{u}^{top} + \dot{v}^{top}\delta\dot{v}^{top} + \dot{w}^{top}\delta\dot{w}^{top})\, dV_{top} \\ &+ (\dot{u}^{core}\delta\dot{u}^{core} + \dot{v}^{core}\delta\dot{v}^{core} + \dot{w}^{core}\delta\dot{w}^{core})\, dV_{core} \\ &+ \int_{V_{bottom}} \rho_{bottom}(\dot{u}^{bottom}\delta\dot{u}^{bottom} + \dot{v}^{bottom}\delta\dot{v}^{bottom} + \dot{w}^{bottom}\delta\dot{w}^{bottom})\, dV_{bottom} \end{aligned} \tag{37}$$

where $\dot{u}, \dot{v}, \dot{w}, V$ and ρ are the micro sandwich beam's velocities in the x, y, and z directions, volume and density, respectively.

The external work includes two parts of the external force and the elastic medium, which are harmonic force and Kerr's foundation, respectively, which are expressed as follows:

$$\delta V = \int_0^A (F_{elastic} - F_{external})\delta w\, dA \tag{38}$$

The resulting force from Kerr's foundation is stated as follows [51, 52]:

$$F_{elastic} = \frac{k_t}{k_t + k_b}\left(k_b w - k_G \frac{\partial^2 w}{\partial x^2}\right) \tag{39}$$

in which k_t, k_b and k_G are top spring, bottom spring and shear layer constants, respectively. Eq. (39) has obtained with details in Appendix A. Also, the resulting force from harmonic force is written as follows:

$$F_{external} = f_0 sin\Omega t \tag{40}$$

where f_0 and Ω are value of force and excited frequency, respectively.

The motion equations of the micro sandwich beam are derived based on MCST and Timoshenko beam theory. By substituting Eqs. (34)-(40) into Eq. (33), the motion equations of core are obtained as follows:

$$\delta\psi: -I^{(2)}\ddot{\psi} + B^{(2)}\psi_{,xx} - k_s C^{(0)}\left(\psi + w_{,x}\right) + \frac{1}{8}G^{(0)}\left(\psi_{,xx} - w_{,xxx}\right) = 0 \tag{41}$$

$$\delta w: -I^{(0)}\ddot{w} + k_s C^{(0)}\left(\psi_{,x} + w_{,xx}\right) + \frac{1}{8}G^{(0)}\left(\psi_{,xxx} - w_{,xxxx}\right) - \frac{k_t}{k_t + k_b}\left(k_b w - k_G w_{,xx}\right) = f_0 sin\Omega t \tag{42}$$

Also, considering the top face sheet as actuator, the motion equations of top face sheet are written as follows:

$$\delta\psi: -I^{(2)}\ddot{\psi} + B^{(2)}\psi_{,xx} - k_s C^{(0)}\left(\psi + w_{,x}\right) + \frac{1}{8}G^{(0)}\left(\psi_{,xx} - w_{,xxx}\right) + 2R^{(2)}\varphi^t_{0,x} + 2R^{(2)}\varphi^b_{0,x} = 0 \tag{43}$$

$$\delta w: -I^{(0)}\ddot{w} + k_s C^{(0)}\left(\psi_{,x} + w_{,xx}\right) + \frac{1}{8}G^{(0)}\left(\psi_{,xxx} - w_{,xxxx}\right) - \frac{k_t}{k_t + k_b}\left(k_b w - k_G w_{,xx}\right) = f_0 sin\Omega t \tag{44}$$

$$\begin{aligned}\varphi^t_0: T^{(2)}\left(\psi_{,x} + w_{,xx}\right) + \left(P^{(4)} - \left(\frac{h_t}{2}\right)^2 P^{(2)}\right)\varphi^t_{0,xx} - \left(\frac{h_t}{2}\right)^2 T^{(0)}\left(\psi_{,x} + w_{,xx}\right) + \left(\frac{h_t}{2}\right)^4 P^{(0)}\varphi^t_{0,xx} - 2R^{(1)}u_{,x} \\ - 2R^{(2)}\psi_{,x} - 4O^{(2)}\varphi^t_0 = \frac{4}{h_t}O^{(1)}V\end{aligned} \tag{45}$$

and considering the bottom face sheet as sensor, the motion equations of bottom face sheet are written as follows:

$$\delta\psi: -I^{(2)}\ddot{\psi} + B^{(2)}\psi_{,xx} - k_s C^{(0)}\left(\psi + w_{,x}\right) + \frac{1}{8}G^{(0)}\left(\psi_{,xx} - w_{,xxx}\right) + 2R^{(2)}\varphi^b_{0,x} = 0 \tag{46}$$

$$\delta w: -I^{(0)}\ddot{w} + k_s C^{(0)}\left(\psi_{,x} + w_{,xx}\right) + \frac{1}{8}G^{(0)}\left(\psi_{,xxx} - w_{,xxxx}\right) - \frac{k_t}{k_t + k_b}\left(k_b w - k_G w_{,xx}\right) = f_0 sin\Omega t \tag{47}$$

$$\begin{aligned}\varphi^b_0: T^{(2)}\left(\psi_{,x} + w_{,xx}\right) + \left(P^{(4)} - \left(\frac{h_b}{2}\right)^2 P^{(2)}\right)\varphi^b_{0,xx} - \left(\frac{h_b}{2}\right)^2 T^{(0)}\left(\psi_{,x} + w_{,xx}\right) + \left(\frac{h_b}{2}\right)^4 P^{(0)}\varphi^b_{0,xx} - 2R^{(1)}u_{,x} \\ - 2R^{(2)}\psi_{,x} - 4O^{(2)}\varphi^b_0 = 0\end{aligned} \tag{48}$$

in which superscript t and b indicate to top and bottom layers, respectively and also, $I^{(i)}$, $B^{(i)}$, $C^{(i)}$, $G^{(i)}$, $R^{(i)}$, $O^{(i)}$ and $T^{(i)}$ are defined:

$$\begin{aligned}I^{(i)} &= \int \rho\, z^{(i)} dz && i = (0, \dots, 6) \\ B^{(i)} &= \int Q_{11}\, z^{(i)} dz && i = (0, \dots, 6) \\ C^{(i)} &= \int Q_{66}\, z^{(i)} dz && i = (0, \dots, 6) \\ G^{(i)} &= \int 2\mu\, l_2^2 z^{(i)} dz && i = (0, \dots, 6) \\ R^{(i)} &= \int e_{31}\, z^{(i)} dz && i = (0, \dots, 6) \\ O^{(i)} &= \int \eta_{33}\, z^{(i)} dz && i = (0, \dots, 6)\end{aligned} \tag{49}$$

$$T^{(i)} = \int e_{15}\, z^{(i)} dz \qquad i = (0, \dots, 6)$$

5. Solution method and control system

The Navier's solution is used to solve the motion equations of the Timoshenko's sandwich micro beam with simply supported obtained as follows:

$$\begin{aligned} \psi(x,t) &= \sum_{n=1}^{\infty} \Psi_0(t) \cos\frac{n\pi x}{L} \\ w(x,t) &= \sum_{n=1}^{\infty} W_0(t) \sin\frac{n\pi x}{L} \\ \phi^t(x,t) &= \sum_{n=1}^{\infty} \Phi^t(t) \sin\frac{n\pi x}{L} \\ \phi^b(x,t) &= \sum_{n=1}^{\infty} \Phi^b(t) \sin\frac{n\pi x}{L} \end{aligned} \tag{50}$$

but, an approach solution is assumed for clamped boundary conditions as follows [7]:

$$\begin{aligned} \psi(x,t) &= \sum_{n=1}^{\infty} \Psi_0(t) f(x) \\ w(x,t) &= \sum_{n=1}^{\infty} \alpha W_0(t) \acute{f}(x) \\ \phi^t(x,t) &= \sum_{n=1}^{\infty} \alpha \Phi^t(t) \acute{f}(x) \\ \phi^b(x,t) &= \sum_{n=1}^{\infty} \alpha \Phi^b(t) \acute{f}(x) \end{aligned} \tag{51}$$

where $\alpha = \frac{-1}{2\lambda_n}$ and $f(x)$ is defined as follows:

$$f(x) = \cos^2(\lambda_n x)\ , \lambda_n = \frac{n\pi}{L} \tag{52}$$

Therefore, the equation obtained in matrix form are written as follows:

$$[\mathrm{M}]\{\ddot{\mathrm{X}}\} + [\mathrm{K}]\{\mathrm{X}\} = -[\mathrm{K_v}]\mathrm{V} + [\mathrm{K_f}]\mathrm{f} \tag{53}$$

where V and f are the applied voltage and force, f is set equal to $f_0 sin\Omega t$ and also the vectors K_v, K_f and X are expressed as follows:

$$\mathrm{K_f} = \begin{Bmatrix} 0 \\ -1 \\ 0 \\ 0 \end{Bmatrix}, \qquad \mathrm{K_v} = \begin{Bmatrix} 0 \\ 0 \\ -\frac{4}{\mathrm{h_t}} \mathrm{O}^{(1)} \\ 0 \end{Bmatrix}, \qquad \mathrm{X} = \begin{Bmatrix} \psi \\ \mathrm{w} \\ \varphi^{\mathrm{t}} \\ \varphi^{\mathrm{b}} \end{Bmatrix} \tag{54}$$

M and K are mass and stiffness matrices for S-S boundary conditions, respectively and the non-zero components m_{ij} and k_{ij} are written as follows:

$$
\begin{aligned}
&m_{11} = -I^{(2)}\\
&m_{22} = -I^{(0)}
\end{aligned}
\tag{55}
$$

$$
\begin{aligned}
&k_{11} = -\left(\frac{n\pi}{l}\right)^2 B^{(2)} - k_s C^{(0)} - \frac{1}{8}\left(\frac{n\pi}{l}\right)^2 G^{(0)}\\
&k_{12} = k_{12} = -\left(\frac{n\pi}{l}\right) k_s C^{(0)} + \frac{1}{8}\left(\frac{n\pi}{l}\right)^3 G^{(0)}\\
&k_{13} = k_{31} = 2\left(\frac{n\pi}{l}\right) R^{(2)} - k_s\left(\frac{n\pi}{l}\right) T^{(2)} + k_s\left(\frac{h_t}{2}\right)^2\left(\frac{n\pi}{l}\right) T^{(0)}\\
&k_{14} = k_{41} = 2\left(\frac{n\pi}{l}\right) R^{(2)} - k_s\left(\frac{n\pi}{l}\right) T^{(2)} + k_s\left(\frac{h_b}{2}\right)^2\left(\frac{n\pi}{l}\right) T^{(0)}\\
&k_{22} = -\left(\frac{n\pi}{l}\right)^2 k_s C^{(0)} + \frac{1}{8}\left(\frac{n\pi}{l}\right)^4 G^{(0)} - \frac{k_t}{k_t + k_b}\left(k_b + k_G\left(\frac{n\pi}{l}\right)^2\right)\\
&k_{23} = k_{32} = -k_s\left(\frac{n\pi}{l}\right)^2 T^{(2)} + k_s\left(\frac{h_t}{2}\right)^2\left(\frac{n\pi}{l}\right)^2 T^{(0)}\\
&k_{24} = k_{42} = -k_s\left(\frac{n\pi}{l}\right)^2 T^{(2)} + k_s\left(\frac{h_b}{2}\right)^2\left(\frac{n\pi}{l}\right)^2 T^{(0)}\\
&k_{33} = -k_s\left(\frac{n\pi}{l}\right)^2 P^{(4)} + k_s\frac{{h_t}^2}{2}\left(\frac{n\pi}{l}\right)^2 P^{(2)} - k_s\left(\frac{h_t}{2}\right)^4\left(\frac{n\pi}{l}\right)^2 P^{(0)} - 4O^{(2)}\\
&k_{44} = -k_s\left(\frac{n\pi}{l}\right)^2 P^{(4)} + k_s\frac{{h_b}^2}{2}\left(\frac{n\pi}{l}\right)^2 P^{(2)} - k_s\left(\frac{h_b}{2}\right)^4\left(\frac{n\pi}{l}\right)^2 P^{(0)} - 4O^{(2)}
\end{aligned}
\tag{56}
$$

Also, the motion equations of active vibration control in the state-space are expressed as following form [53]:

$$
\begin{aligned}
&\mathcal{L} = \begin{pmatrix} X \\ \dot{X} \end{pmatrix}, \dot{\mathcal{L}} = \begin{pmatrix} \dot{X} \\ \ddot{X} \end{pmatrix}\\
&\ddot{X} = M^{-1} \times \left[-\mathrm{K}X + K_v V + K_f f\right]\\
&\dot{\mathcal{L}} = \begin{bmatrix} 0_{2\times2} & I_{2\times2} \\ -M^{-1}K & 0_{2\times2} \end{bmatrix}\mathcal{L} + \begin{bmatrix} 0_{2\times2} \\ M^{-1}K_v \end{bmatrix} V + \begin{bmatrix} 0_{2\times2} \\ M^{-1}K_f \end{bmatrix} f\\
&\begin{cases} \dot{\mathcal{L}} = A\mathcal{L} + BV + Cf \\ Y = D\mathcal{L} \end{cases}
\end{aligned}
\tag{57}
$$

Therefor

$$A = \begin{bmatrix} 0_{2\times2} & I_{2\times2} \\ -M^{-1}K & 0_{2\times2} \end{bmatrix}$$

$$B = \begin{bmatrix} 0_{2\times2} \\ -M^{-1}\mathrm{K}_v \end{bmatrix}$$

$$C = \begin{bmatrix} 0_{2\times2} \\ M^{-1}K_f \end{bmatrix}$$

$$D = \begin{bmatrix} \cos\frac{n\pi x}{L} & 0 & 0 & 0 \\ 0 & \sin\frac{n\pi x}{L} & 0 & 0 \end{bmatrix}$$

To control the vibration of structure, due to the linearity of the state-space equations, state-feedback controller is determined based on LQR. The optimal actuator voltage is obtained based on LQR approach, therefore the cost function include voltage is determined as follows [54]:

$$J = \frac{1}{2}\int_0^\infty (\mathcal{L}^T Q \mathcal{L} + \mathrm{V}^T R \mathrm{V}) dt \quad (1)$$

in which R and Q are weight matrix that are positive-definite and positive semi-definite, respectively. The optimal voltage and state-feedback gain matrix are written as following form [55]:

$$\mathrm{V} = -\mathrm{G_v} \times \mathcal{L} \quad (2)$$

$$G_v = R^{-1} B^T P \quad (3)$$

To optimal state-space gain matrix, P is obtained from solving the algebraic Riccati equation as follows [56]:

$$A^T P + PA - PBR^{-1}B^T P + Q = 0 \quad (4)$$

6. Validation and numerical result

6.1. Validation

Three modes of dimensionless natural frequency of Timoshenko micro beam are compared by Akgöz and Civalek [57] and the results are presented in Table 1, Table 2 and Table 3. For this purpose, a simply supported Timoshenko micro beam is considered with rectangular cross-section (shear correction factor is $k_s = 5/6$) and for different length to thickness ratio ($L/h = 10, 30\ and\ 100$), the width to thickness ratio is constant (b/h=2). The Timoshenko micro beam is considered based on MCST, and material properties and length scale parameter are as follows [57]:

$$E = 1.44\ Gpa, \rho = 1220\ {}^{kg}/_{m^3}\ , \nu = 0.3\ , l_2 = 17.6\ \mu m \quad (5)$$

As a reminder, the MSCT will be turned into the CT if the material length parameter is equal zero. As shown in the Table 1, Table 2 and Table 3, for all of length to thickness ratio ($L/h = 10, 30\ and\ 100$) and three of thickness to small scale parameter ($h/l = 1, 5\ and\ 10$) and also, for three modes of first dimensionless natural frequency in CT and MCST, the present work have very high agreement with literature and the error is approximately near to zero. Thus it is shown that the obtained equations of present work have good accuracy.

Table 1. Comparison of first mode dimensionless natural frequency of Timoshenko beam theory (TBT) based classical theory (CT) and Modified couple stress theory (MCST) ($\bar{\omega} = \omega_1 L^2 \sqrt{\rho A/EI}$).

h/l	Theory		L/h=10	L/h=30	L/h=100
1	CT	Bekir Akgöz [57]	13.1232	13.4595	13.4996
		Present work	13.123178	13.459454	13.499630
	MCST	Bekir Akgöz [57]	23.7053	24.5061	24.6045
		Present work	23.705256	24.506058	24.604512
5	CT	Bekir Akgöz [57]	13.1232	13.4595	13.4996
		Present work	13.123178	13.459454	13.499630
	MCST	Bekir Akgöz [57]	13.7192	14.0707	14.1128
		Present work	13.719171	14.070713	14.112778
10	CT	Bekir Akgöz [57]	13.1232	13.4595	13.4996
		Present work	13.123178	13.459454	13.499630

	MCST	Bekir Akgöz [57]	13.2748	13.6149	13.6555
		Present work	13.274809	13.614857	13.655500

Table 2. Comparison of second mode dimensionless natural frequency of Timoshenko beam theory (TBT) based classical theory (CT) and Modified couple stress theory (MCST) $(\bar{\omega} = \omega_1 L^2\sqrt{\rho A/EI})$

h/l	Theory		L/h=10	L/h=30	L/h=100
1	CT	Bekir Akgöz [57]	48.6751	53.3195	53.9507
		Present work	48.675128	53.319531	3.950666
	MCST	Bekir Akgöz [57]	86.4924	96.7708	98.3005
		Present work	86.492440	96.770790	98.300516
5	CT	Bekir Akgöz [57]	48.6751	53.3195	53.9507
		Present work	48.675128	53.319531	3.950666
	MCST	Bekir Akgöz [57]	50.9056	55.7406	56.4010
		Present work	50.905625	55.740590	56.401002
10	CT	Bekir Akgöz [57]	48.6751	53.3195	53.9507
		Present work	48.675128	53.319531	3.950666
	MCST	Bekir Akgöz [57]	49.2437	53.9352	54.5736
		Present work	49.243735	53.935218	54.573587

Table 3. Comparison of third mode dimensionless natural frequency of Timoshenko beam theory (TBT) based classical theory (CT) and Modified couple stress theory (MCST) $(\bar{\omega} = \omega_1 L^2\sqrt{\rho A/EI})$

h/l	Theory		L/h=10	L/h=30	L/h=100
1	CT	Bekir Akgöz [57]	98.8865	118.1086	121.2103
		Present work	98.886538	118.108608	121.210274
	MCST	Bekir Akgöz [57]	174.0724	213.3473	220.7383
		Present work	174.072424	213.347312	220.738314
5	CT	Bekir Akgöz [57]	98.8865	118.1086	121.2103
		Present work	98.886538	118.108608	121.210274
	MCST	Bekir Akgöz [57]	103.5636	123.4725	126.7151
		Present work	103.563559	123.472540	126.715135
10	CT	Bekir Akgöz [57]	98.8865	118.1086	121.2103
		Present work	98.886538	118.108608	121.210274
	MCST	Bekir Akgöz [57]	100.0818	119.4733	122.6098
		Present work	100.081806	119.473282	122.609772

6.2. Numerical results

The material properties, dimension, and elastic foundation of Timoshenko micro sandwich beam with three-phase nanocomposite/piezoelectric/resin as face sheet, which are top and bottom face sheet as actuator and sensor, respectively, as follows [31, 45, 58]:

$$E_{core} = 115\ Gpa, \nu_{core} = 0.3, \rho_{core} = 199\ {}^{kg}/_{m^3}, E_{resin} = 2.72\ Gpa, \rho_{resin} = 1200\ {}^{kg}/_{m^3}, \nu_{resin} = 0.33, E_{11PVDF} = 238\ Gpa, E_{22PVDF} = 23.6\ Gpa, \rho_{PVDF} = 1750\ {}^{kg}/_{m^3}, \nu_{PVDF} = 0.18, e_{31} = -0.13\ {}^{C}/_{m^2}, e_{15} = -0.01\ {}^{C}/_{m^2}, \eta_{11} = 11.0625 \times 10^{-9}\ {}^{C^2}/_{Nm^2}, \eta_{33} = 10.6023 \times 10^{-9}\ {}^{C^2}/_{Nm^2}, V_{PVDF} = 0.55, E_{CNT} = 640\ Gpa, \rho_{CNT} = 1350\ {}^{kg}/_{m^3}, \nu_{CNT} = 0.33, t_{CNT} = 0.34\ nm, d_{CNT} = 1.4\ nm, l_{CNT} = 25\ \mu m, E_{GPL} = 1010\ Gpa, \rho_{GPL} = 1060\ {}^{kg}/_{m^3}, \nu_{GPL} = 0.186, w_{GPL} = 1.5\ \mu m, h_{CNT} = 1.5\ nm, l_{GPL} = 2.5\ \mu m, l_2 = 17.6\ \mu m, h_t = h_b = 0.1h, L = 8h, h = 2l_2, b = {}^{1}/_{4}\ h \tag{6}$$

Also, the properties material of CNR is obtained from the following temperature-dependent relationship [44]:

$$E_{11CNR} = 0.76798 - 5.2061 \times 10^{-4}T + 8.916 \times 10^{-7}T^2 - 0.535 \times 10^{-9}T^3\ Tpa$$
$$E_{22CNR} = 0.962586 - 6.50445 \times 10^{-4}T + 11.13 \times 10^{-7}T^2 - 0.6675 \times 10^{-9}T^3\ Tpa \tag{7}$$
$$\rho_{CNR} = 1550\ {}^{kg}/_{m^3}, \nu_{CNR} = 0.19$$

In this research, the material properties of CNR is considered in environment temperature ($300^0 K$).

In order to investigate the effect of various types of nanocomposites on the active control of forced vibrations of Timoshenko's sandwich micro beam under harmonic force, three types of nanocomposites CNT, CNR and GPL are considered for face sheets with different volume fractions. Also, excitation frequency and value of harmonic force for all of results is assumed as the first natural frequency and 0.01N, respectively. Fig.2a,b illustrates the frequency response of forced vibration and deflection response and settling time for various volume fractions of Timoshenko's micro sandwich beam, respectively. As seen in Fig.2 by increasing volume fraction, the frequency is increased and deflection is decreased. Also, settling time is decreased and oscillations reduction is occurred earlier.

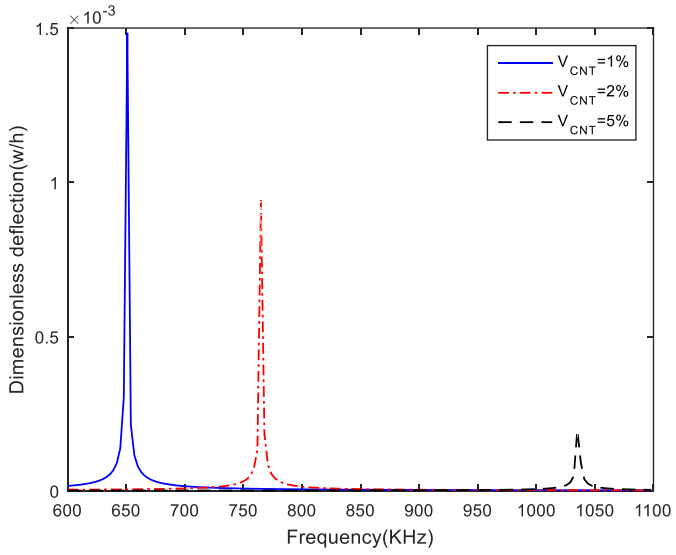

(a)

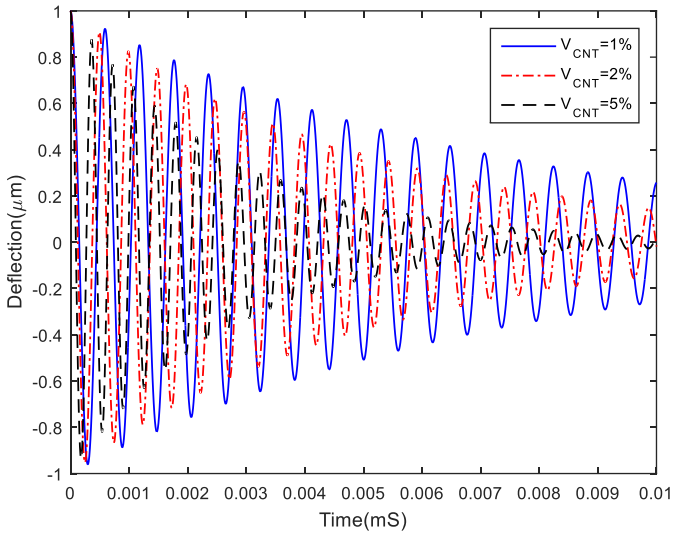

(b)

Fig.2. a) Frequency response of forced vibration and b) Settling time of various CNT volume fractions of Timoshenko's sandwich micro beam

In optimal control, the system can be controlled by optimizing its variables, the optimized variable or function is called the cost function and minimizing the cost function can control system inputs. The cost function is the square of system state variables and control inputs. Therefore, the cost function is defined as equation (58) and considering the weight matrices R and Q, respectively positive-definite and positive semi-definite, the cost function is non-negative and its minimum value becomes zero. Thus, the state variables and control inputs tend to zero, which is favorable for the studied system. The values considered for Q and R express the importance of state variables and control inputs. According to the importance of each variable and, a weight factor is considered, and each variable that is more important in the optimization problem has a higher weight factor. In the desired system, which is a Timoshenko's micro sandwich beam reinforced nanocomposite integrated by piezoelectric layers, their selection depends on the characteristics of the system, where R can be considered as a unit step and Q is proportional to the mass and stiffness matrices. Then using solving the algebraic Riccati equation by MATLAB software, optimum control gain is obtained and the control input is also optimized.

Dimensionless deflection versus frequency and deflection versus time of Timoshenko's micro sandwich beam with foam core and GPLs reinforced composite integrated by piezoelectric (PVDF) as face sheets are showed in Fig.3a,b. As can be seen, increasing the volume fraction of GPLs increases the natural frequency and decreases the deflection amplitude and settling time.

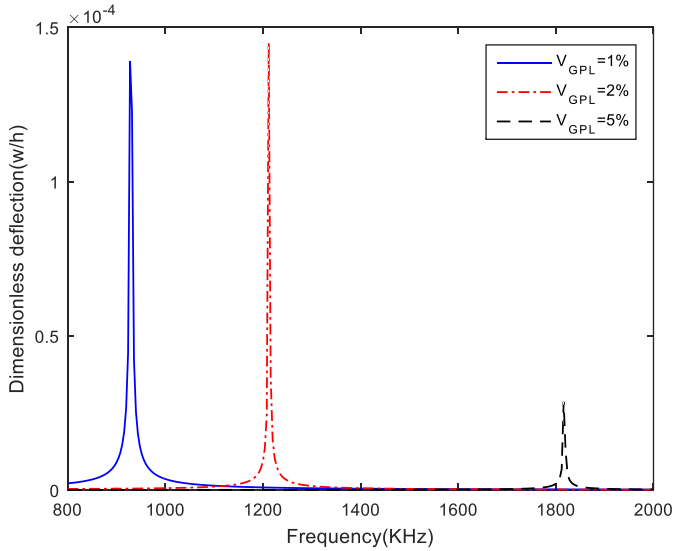

(a)

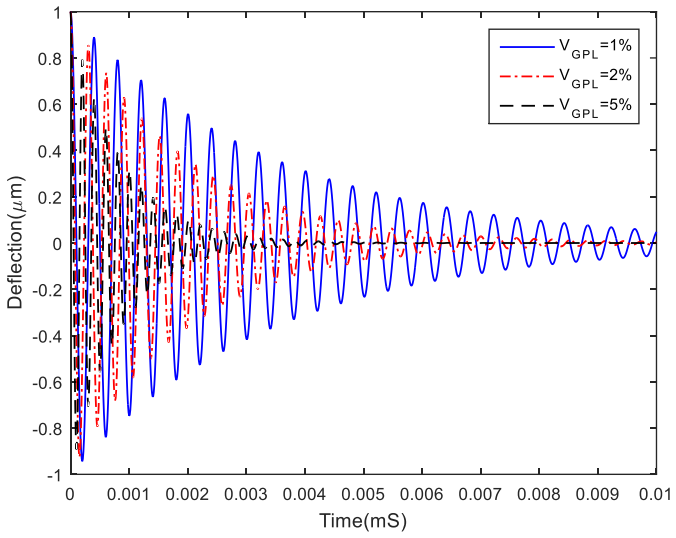

(b)

Fig.3. a) Frequency response of forced vibration and b) Settling time of various GPL volume fractions of Timoshenko's sandwich micro beam

Fig.4a,b indicates resonance frequency and deflection of Timoshenko's micro sandwich beam for various volume fractions of CNR. It shows that with the increase of the volume fraction, the natural frequency increases and the deflection decreases, and as a result, the vibrations of the structure are suppressed faster.

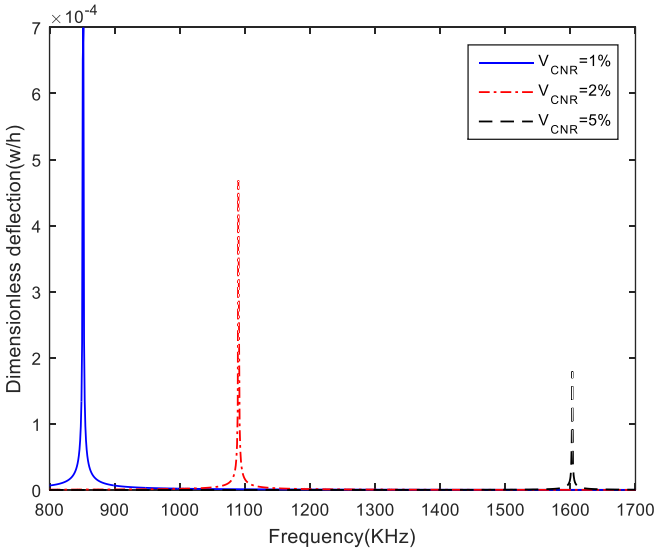

(a)

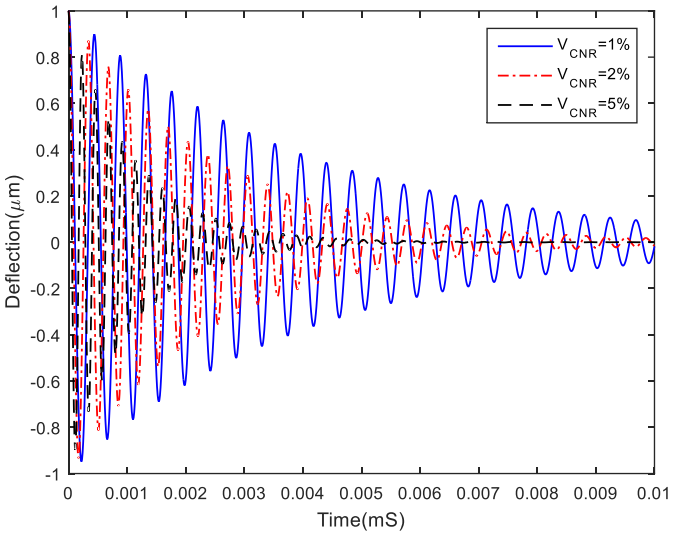

(b)

Fig.4. a) Frequency response of forced vibration and b) Settling time of various CNR volume fractions of Timoshenko's sandwich micro beam

By comparing Fig.2, Fig.3 and Fig.4, it can be seen that in three type of nanocomposite reinforced by CNT, GPL and CNR, the natural frequency increases with the increase in volume fraction of nanocomposites. It is clearly evident that since the nanocomposites have a high modulus of elasticity and increasing volume fraction increases the stiffness of the structure, therefore the natural frequency which depends on the stiffness increases. Also, increasing volume fraction of nanocomposite and stiffness of Timoshenko's micro sandwich beam decreases the amplitude of the deflection center point, so attenuation of the deflection response becomes faster.

Now, after analysis of deflection response and settling time of various volume fractions of nanocomposite reinforced, the frequency and deflection response of nanocomposite reinforced of CNT, GPL and CNR are analyzed to find the nanocomposite reinforced with the shortest settling time of the Timoshenko's micro sandwich beam. Fig.5a,b, respectively, display forced vibrations and deflection response of three type of nanocomposite reinforced for a Timoshenko's micro sandwich beam that face sheets are reinforced with nanocomposites (CNT or GPL or CNR) integrated by piezoelectric for volume fraction 1%. As can be seen, the natural frequency of CNT is less than CNR and GPL, respectively. Also, vibrations damping and settling time of GPL is faster than CNR and CNT, respectively.

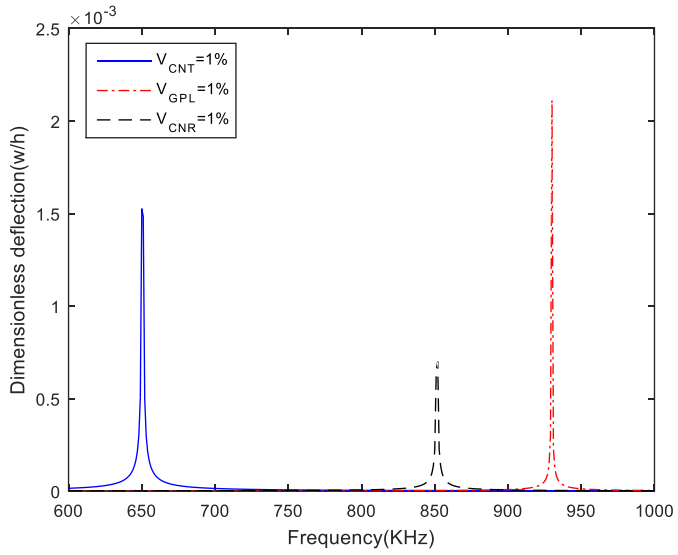

(a)

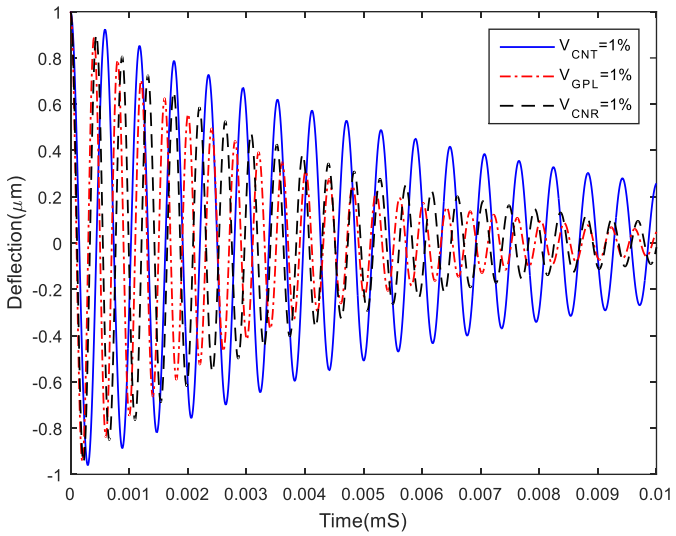

(b)

Fig.5. a) Frequency response of forced vibration and b) deflection response of three type of CNT/GPL/CNR reinforced nanocomposite for Timoshenko's sandwich micro beam

According to the natural frequency is depends on stiffness and in this research, Young modulus of CNT is lower than CNR and GPL, respectively. Therefore, Timoshenko's micro beam that are reinforced CNT nanocomposite integrated by piezoelectric as face sheet and foam core has lower natural frequency. Also, structure with more stiffness has less deflection. Therefore, the amplitude of the center point deflection and settling time for Timoshenko's sandwich micro beam with GPL reinforced is lower and earlier than the other two nanocomposites, respectively.

The First three natural frequencies of various nanocomposite reinforcements (CNT, GPL and CNR) with various volume fractions for Timoshenko's micro sandwich beam are shown in Table 4a,b. In realistic scenarios, it has been shown that the presence of nanocomposites in the structure significantly increases in flexural modulus, Young's modulus and inter-laminar shear strength [59]. Also, in the experimental studies, fracture-mechanical properties are investigated, it has been shown that the addition of a small amount of nanocomposite is significantly improved strain to failure and fracture toughness [60]. It has also been shown in other studies that with the increase in volume fraction of nanocomposites and natural frequency modes, the value of critical buckling load increases [8]. Therefore, Table 4b shows the effect of increasing the different volume fractions (1, 2 and 5) on the first natural frequency modes are compared to without considering reinforcement. As can be seen, for CNT nanocomposite with increasing of volume fraction up to 1%, the first mode of natural frequency is increased by about 27.6%, which is by about 82.4% for GPL and by about for 67% CNR. Also, by increasing volume fraction up to 1%, the second mode of natural frequency is increased by about 28.9% for CNT, 85.8% for GPL and 69.9% for CNR and also, the third mode of natural frequency is increased by about 30%, 88.6% and 72.3% for CNT, GPL and CNR, respectively. For Timoshenko's micro sandwich beam with CNT reinforced integrated by piezoelectric, the second and third modes of natural frequency of the various volume fractions (1%, 2% and 5%) are increased by about 3.5 and 6.6 times, respectively, compared to the first mode of natural frequency, which are by about 3.5 and 6.7 times for GPL and 3.5 and 6.7 for CNR. As a result, for the volume fraction 1%, 2% and 5%, the second and third modes of natural frequency increase the frequency with a constant amount for three nanocomposite CNT, GPL and CNR.

Individual influence of CNT, GPL, and CNR on first three natural frequency of Timoshenko's micro sandwich beam for various volume fraction of nanocomposite reinforcements is shown in Table 4a. By comparing the first and second columns of Table 4a, by adding 1% nanocomposite (CNT, CNR and GPL), the stiffness of the structure increases and as a result the natural frequency increases. Also, in Table 4b, it is shown that with increasing of 1% reinforcements (CNT,GPL, and CNR), the natural frequency enhances 27.61%, 82.41%, and 67.04% for first natural frequency, respectively. On the other hands, the effect of GPL on the natural frequency is higher than other reinforcemnts. Individual influence of nanocomposites on damping characteristics is indicated in Fig 6. As can be seen, by adding CNT to Timoshenko's micro sandwich beam, the stiffness of structure is increased and as a result amplitude of deflection is reduced and a faster settling time is obtained.

Table 4. a) Comparison of first three natural frequency modes of Timoshenko's micro sandwich beam for various volume fraction of nanocomposite reinforcements.

Natural frequencies modes (KHz)	Nanocomposite	Volume fractions			
		Without considering reinforcement	1%	2%	5%
1st mode	CNT	509.7700	650.4932	765.4926	1035.9495
	GPL	509.7700	929.8766	1212.8146	1817.2365
	CNR	509.7700	851.5180	1090.3433	1602.7200
2nd mode	CNT	1730.5131	2231.1110	2636.7761	3585.5724
	GPL	1730.5131	3214.6215	4205.6336	6318.8759
	CNR	1730.5131	2939.6985	3777.2872	5569.9761
3rd mode	CNT	3271.2166	4253.0795	5044.3388	6887.5101
	GPL	3271.2166	6168.6256	8091.5053	12186.0939
	CNR	3271.2166	5634.5413	7261.4473	10737.2181

b) The effect of enhancement percentage for different volume fractions on the first three natural frequency compared to the case without considering reinforcement

Natural frequencies modes (KHz)	Nanocomposite	Volume fractions			
		Without considering reinforcement	1%	2%	5%
1st mode	CNT	509.7700	27.61%	50.16%	103.22%
	GPL	509.7700	82.41%	137.91%	256.48%
	CNR	509.7700	67.04%	113.89%	214.40%
2nd mode	CNT	1730.5131	28.93%	52.37%	107.20%
	GPL	1730.5131	85.76%	143.03%	265.14%
	CNR	1730.5131	69.87%	118.28%	221.87%
3rd mode	CNT	3271.2166	30.02%	54.20%	110.55%
	GPL	3271.2166	88.57%	147.35%	272.52%
	CNR	3271.2166	72.25%	121.98%	228.23%

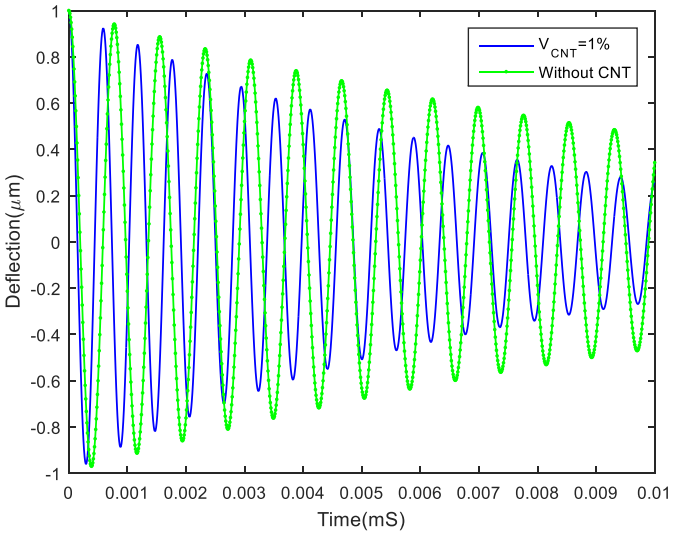

(a)

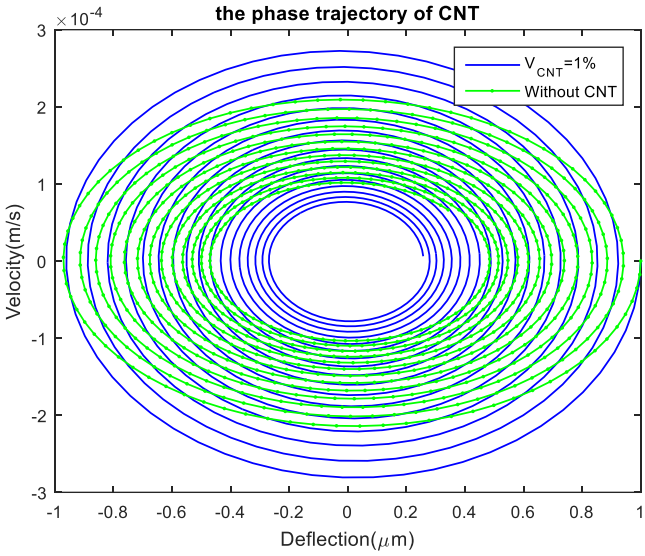

(b)

Fig.6. Influence adding of CNT on a) settling time and b) the phase trajectory of Timoshenko's micro sandwich beam

In the following, the active vibrations control of Timoshenko's micro sandwich beam with foam as core and CNR reinforced integrated by piezoelectric as face sheets on Kerr's foundation is investigated and the effects of top and bottom springs and shear layer constant on forced frequency response and settling time for volume fraction 1% is indicated in Fig.7a,b. Also, springs coefficient and shear layer constant are considered dimensionless as following form:

$$k_t^* = \frac{k_t L}{B^{(0)}} \tag{8}$$

$$k_b^* = \frac{k_b L}{B^{(0)}} \tag{9}$$

$$k_G^* = \frac{k_G}{B^{(0)} L} \tag{10}$$

and k_t^* , k_b^* and k_G^* are considered equal to 1000, 1000 and 100.

As reminder, according to equation of Kerr's foundation (39), foundation is Pasternak if k_t tend to infinity, foundation is Winkler if k_t tend to infinity and k_G to be zero, structure is without foundation if k_b and k_G to be zero (here without foundation means simply support) [61].

As can be seen in Fig.7a, natural frequency of Pasternak foundation is more than Kerr foundation and Winkler foundation and without foundation, respectively. Fig.7b displays that the amplitude of center point deflection of Pasternak foundation is greater than Kerr, Winkler and without foundation and also settling time of Pasternak foundation is slower. Due to related Kerr foundation, for same spring coefficient, spring coefficient of Kerr foundation is less than Pasternak, therefore, stiffness of structure on Pasternak foundation is clearly more than Kerr foundation, Winkler and without foundation. In result, the frequency response and settling time of Pasternak foundation are larger and slower, respectively. Therefore, for active control of Timoshenko's micro sandwich beam, the Kerr foundation is better than Pasternak foundation. As a general result, it can be stated that increasing the stiffness of structure increases the frequency response and decreases the settling time and the transient response of deflection.

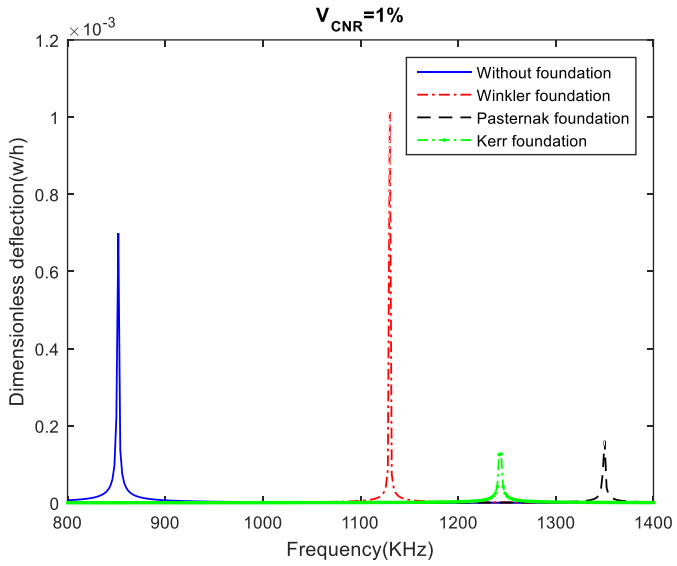

(a)

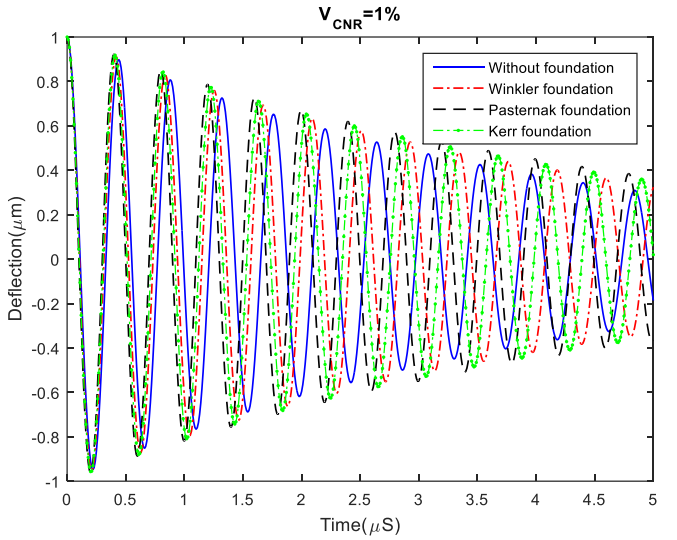

(b)

Fig.7. a) Frequency response of forced vibration and b) deflection response of Timoshenko's sandwich micro beam on various foundation

Table 5 shows the first, second and third mode of natural frequency of Timoshenko's micro sandwich beam with CNR reinforced nanocomposite integrated by piezoelectric on Kerr foundation, where the three parameters of foundation (k_t, k_b and k_g) are varied. the first, second and third mode of natural frequency of the Kerr foundation is increased by about 46%, 13.1% and 7.7%, respectively, compared to without foundation and by about 10%, 9.7% and 6.8%, respectively, compared to Winkler foundation. Also, the first, second and third mode of natural frequency of the Kerr foundation are decreased by about 8.6%, 1.2% and 0.3%, respectively, compared to Pasternak foundation.

Table 5. Comparison of three natural frequency modes for various foundation of Timoshenko's micro sandwich beam with CNR reinforced integrated by piezoelectric (Volume fraction of CNR=1%)

Natural frequency modes (KHz)	Kerr	Pasternak	Winkler	Without foundation
1st mode	1243.0074	1349.3600	1129.8420	851.5180
2nd mode	3323.9479	3364.3886	3030.3549	2939.6985
3rd mode	6067.5883	6089.7916	5682.2842	5634.5413

Fig.8a,b shows dimensionless deflection versus frequency and deflection versus time of three modes of natural frequency for Timoshenko's micro sandwich beam on Kerr's foundation with face sheets are reinforced by CNR integrated by piezoelectric. In the forced vibration response for volume fraction 1%, the natural frequency increases with

increasing mode of natural frequency. Also, by increasing mode of natural frequency, the amplitude of deflection is increased and damping of vibrations is delayed.

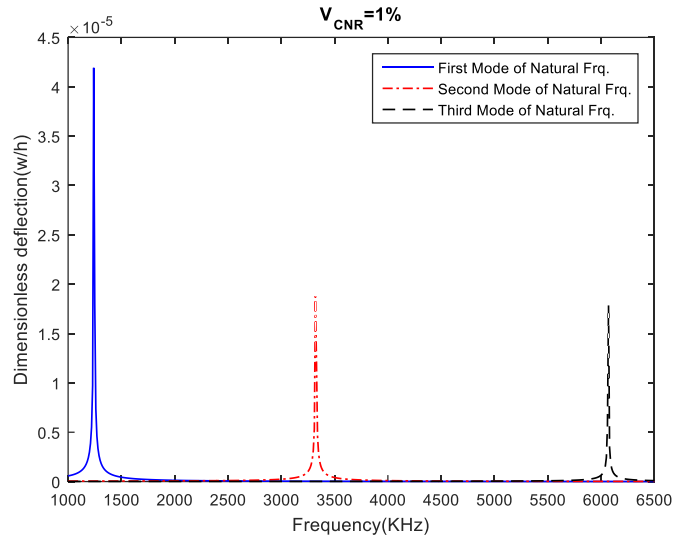

(a)

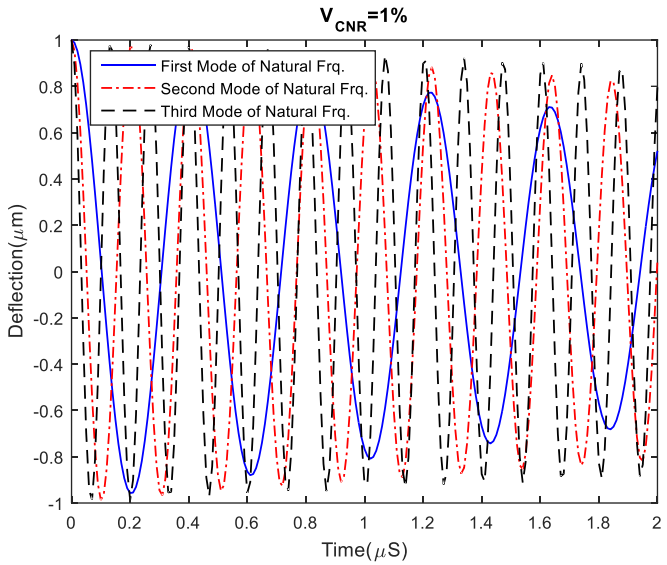

(b)

Fig.8. a) Frequency response of forced vibration and b) deflection response of Timoshenko's sandwich micro beam for three modes of natural frequency

Because the sandwich beam becomes at micro scale, it is very important to use material length scale parameter that can correctly increase the stiffness of a sandwich beam in vibration control. One of the theories becomes modified couple stress theory (MCST) that considers the effect of material length scale parameter and can correctly enhance the stiffness of the structure. Figs. 9a and b show the first natural frequency and deflection response of Timoshenko's micro sandwich beam with CNT reinforced nanocomposite integrated by piezoelectric for classical theory (CT) and MCST. It is shown that the stiffness structure in MCST is more than in CT, so the natural frequency is higher. But, the amplitude of center point deflection and settling time of structure in MCST is slightly changed compared to CT.

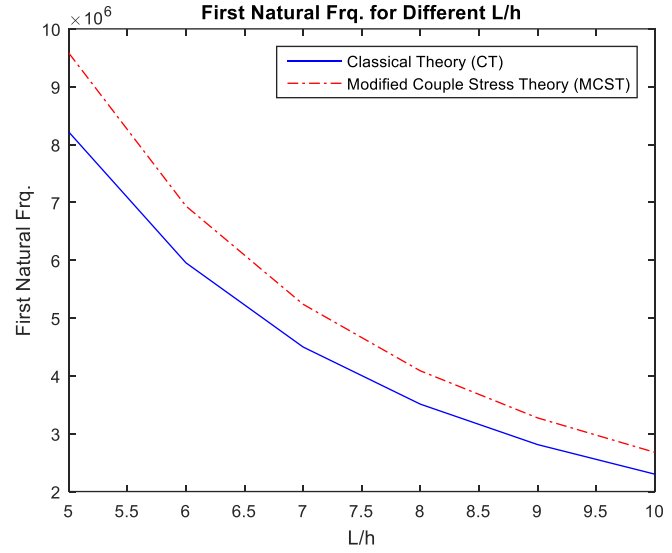

(a)

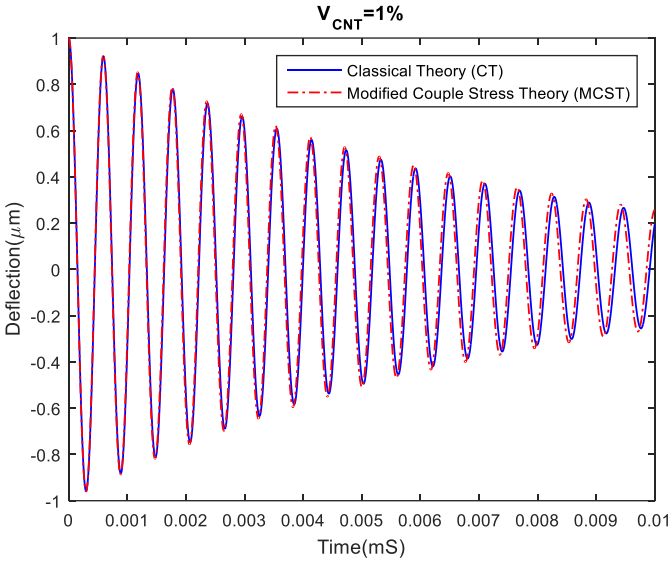

(b)

Fig.9. a) The first natural frequency versus different L/h and b) deflection versus time of CT and MCST for Timoshenko's micro sandwich beam reinforced CNT integrated by piezoelectric layers

Fig. 10 shows the effect of two types of boundary conditions (simply supported (S-S) and clamped (C-C)) on the natural frequency of Timoshenko's micro sandwich beam reinforced CNT integrated piezoelectric layers. It is shown that the natural frequency for C-C BC's is higher that of S-S BC's, because the stiffness of structure for C-C is more than the other BC's.

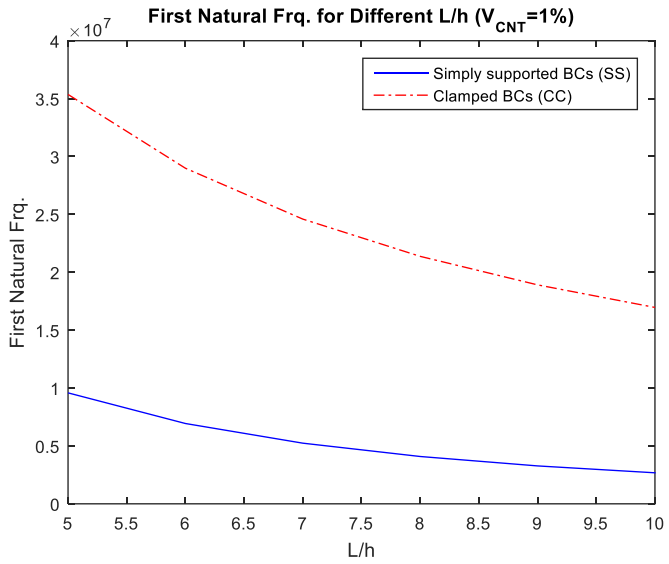

Fig.10. The effect of two types of boundary conditions (S-S and C-C) on the natural frequency of Timoshenko's micro sandwich beam reinforced CNT integrated piezoelectric layers

The beating phenomenon occurs when the excitation frequency of the applied harmonic force is very close to the natural frequency of the structure, but not exactly equal to it. Fig.11 shows forced vibration control of Timoshenko's micro sandwich beam reinforced CNT integrated piezoelectric with excited frequency near the natural frequency.

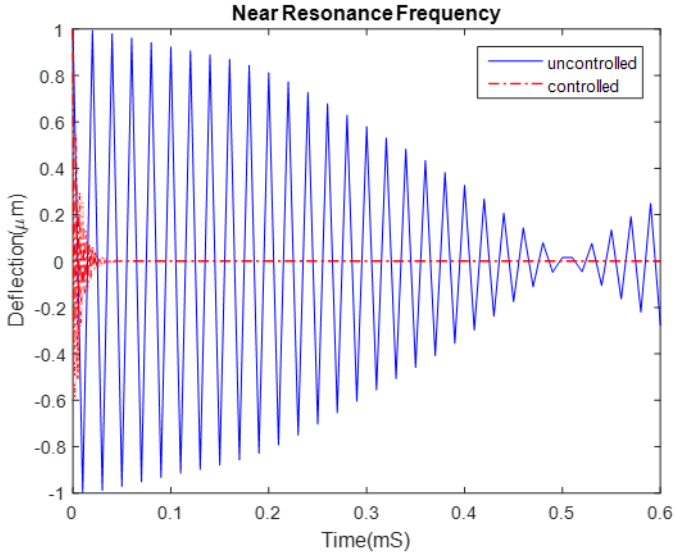

Fig.11. Forced vibration control of Timoshenko's micro sandwich beam with CNT reinforced integrated piezoelectric and excited frequency equal 97% natural frequency

7. Conclusion

In this research, the active control of forced vibrations of Timoshenko's micro sandwich beam with foam core. Three types of CNT, CNR and GPL nanocomposite reinforcements integrated by piezoelectric are assumed for face sheets. Top and bottom face sheet was considered as actuator and sensor, respectively, and the micro sandwich structure was rested on Kerr's foundation. Timoshenko beam theory based on MCST was used to derive the governing equations. The active control of vibrations was achieved using state space form and LQR approach. After validation of motion equations, effects of various volume fraction of CNTs/GPLs/CNRs on forced vibration response and amplitude of deflection center point and settling time were analyzed and also, difference between CNT, GPL and CNR and also various modes of natural frequency in reducing vibrations was investigated. The effect of spring coefficients and shear layer constant of Kerr foundation on vibration attenuation and natural frequency was analyzed. The results following can be obtained from this research:

- The beating phenomenon have considered in the present work that these phenomenon occurs when the excitation frequency of the applied harmonic force is very close to the natural frequency of the structure, but not exactly equal to it.

- Increasing volume fraction of nanocomposite reinforcements increases natural frequency and decreases settling time and amplitude of deflection.

- By comparing the natural frequency and settling time of similar volume fraction of CNT, GPL and CNR reinforced composite, GPLs had highest natural frequency and lowest settling time and amplitude of center point deflection.

- Among the two elastic foundation of Kerr and Pasternak, the natural frequency and settling time of Kerr foundation are less than Pasternak foundation.

- By increasing the stiffness of the structure, natural frequency was increased and settling time was decreased and vibrations attenuation was occurred sooner.

- Increasing the natural frequency mode increases force vibration response and amplitude of deflection and settling time.

- The second mode of natural frequency was increased by about 3.6 times compared to the first mode of natural frequency for various volume fractions of CNT, GPL and CNR.

- The third mode of natural frequency was increased by about 7 times compared to the first mode of natural frequency for various volume fractions of CNT, GPL and CNR.

- The Kerr foundation was increased the natural frequency more than Winkler foundation and less than Pasternak foundation.

- For constant spring coefficient, the amplitude of center point deflection of Kerr foundation was less than Pasternak foundation and more than Winkler foundation. Also the settling time of Kerr foundation was faster than Pasternak foundation and slower than Winkler foundation.

- It is shown that with adding 1% reinforcements (CNT,GPL, and CNR), the first natural frequency enhances 27.61%, 82.41%, and 67.04%, respectively.

- It is shown that the natural frequency for C-C BC's is higher that of S-S BC's, because the stiffness of structure for C-C is more than the S-S BC's.

- Because the sandwich beam becomes at micro scale, it is very important to use material length scale parameter that can correctly increase the stiffness of a sandwich beam in vibration control. The first natural frequency and deflection response of Timoshenko's micro sandwich beam with CNT reinforced nanocomposite integrated by piezoelectric for classical theory (CT) and MCST are considered. It is shown that the stiffness structure in MCST is more than in CT, so the natural frequency increases more. But, the amplitude of center point deflection and settling time of structure in MCST is slightly changed compared to CT.

Acknowledgments

The authors would like to thank the referees for their valuable comments and also thank a lot for increasing the quality of the present work.

References

[1] S. Moradi Haghighi, A. Alibeigloo, Thermal Buckling and Vibrational Analysis of Carbon Nanotube Reinforced Rectangular Composite Plates Based on Third-Order Shear Deformation Theory, *Journal of Engineering Mechanics*, Vol. 149, No. 6, pp. 04023026, 2023/06/01, 2023.

[2] J. Zheng, C. Zhang, F. Musharavati, A. Khan, T. A. Sebaey, Thermo-mechanical buckling analysis of FG-GNPs reinforced composites sandwich microplates using a trigonometric four-variable shear deformation theory, *Case Studies in Thermal Engineering*, Vol. 26, pp. 101120, 2021/08/01/, 2021.

[3] A. Mihankhah, Z. Khoddami Maraghi, A. Ghorbanpour Arani, Vibration and aeroelastic instability analysis in GPL-porous multi-layered beam with the rotation effect, *International Journal for Computational Methods in Engineering Science and Mechanics*, pp. 1-24.

[4] M. Karimiasl, A. Alibeigloo, Nonlinear vibration characteristic of a sandwich cylindrical panel with auxetic core and GPLRC facing sheets embedded with piezoelectric layers, *Journal of Intelligent Material Systems and Structures*, Vol. 34, No. 10, pp. 1159-1177, 2023/06/01, 2022.

[5] F. Bargozini, M. Mohammadimehr, E. A. Dawi, M. Salavati-Niasari, Buckling of a sandwich beam with carbon nano rod reinforced composite and porous core under axially variable forces by considering general strain, *Results in Engineering*, Vol. 21, pp. 101945, 2024/03/01/, 2024.

[6] A. Noruzi, M. Mohammadimehr, F. Bargozini, Experimental and theoretical results for bending and buckling of a five-layer sandwich plate reinforced by carbon nanotubes/carbon nanorods/graphene platelets/shape memory alloy based on RFSDT, *Archive of Applied Mechanics*, Vol. 94, No. 8, pp. 2151-2173, 2024/08/01, 2024.

[7] M. Pahlavanzadeh, M. Mohammadimehr, M. Irani-Rahaghi, S. M. Emamat, Vibration response on the rod of vortex bladeless wind power generator for a sandwich beam with various face sheets and cores based on different boundary conditions, *Mechanics Based Design of Structures and Machines*, pp. 1-27.

[8] M. Arabzadeh-Ziari, M. Mohammadimehr, E. Arabzadeh-Ziari, M. Asgari, Deflection, buckling and vibration analyses for a sandwich nanocomposite structure with foam core reinforced with GPLs and SMAs based on TSDBT, *Journal of Computational Applied Mechanics*, Vol. 55, No. 2, pp. 289-321, 2024.

[9] R. Kumar, M. Singh, C. Kumar, J. Damania, J. Singh, J. Singh, Assessment of Radial basis function based meshfree method for the buckling analysis of rectangular FGM plate using HSDT and Strong form formulation, *Journal of Computational Applied Mechanics*, Vol. 53, No. 3, pp. 332-347, 2022.

[10] E. Arabzadeh-Ziari, M. Mohammadimehr, M. Arabzadeh-Ziari, M. Asgari, Vibration, Bending, and Buckling of a Seven-Layer Sandwich Beam with Balsa Core Reinforced by Nanocomposite and Shape Memory Alloy Face Sheets Using Piezoelectromagnetic Layers, *Arabian Journal for Science and Engineering*, 2024/09/06, 2024.

[11] E. Sh Khoram-Nejad, S. Moradi, M. Shishesaz, Free vibration analysis of the cracked post-buckled axially functionally graded beam under compressive load, *Journal of Computational Applied Mechanics*, Vol. 52, No. 2, pp. 256-270, 2021.

[12] S. R. Bathini, V. K. R. K, C. A. B, Free vibration behavior of bi-directional functionally graded plates with porosities using a refined first order shear deformation theory, *Journal of Computational Applied Mechanics*, Vol. 51, No. 2, pp. 374-388, 2020.

[13] Y. Zhao, F. Guo, D. Xu, Vibration energy characters study of a soft-core beam system coupled through nonlinear coupling layers, *Communications in Nonlinear Science and Numerical Simulation*, Vol. 129, pp. 107681, 2024.

[14] Z.-Y. Li, L.-T. Xie, T.-X. Ma, Y.-Z. Wang, Y.-Y. Chai, C. Zhang, F.-M. Li, A simple active adaptive control method for mitigating and isolating mechanical vibrations of the pyramid-core lattice sandwich structures, *Journal of Sound and Vibration*, Vol. 577, pp. 118321, 2024.

[15] J. Morales, R. Sedaghati, A Novel Semi-Active Control Approach for Flexible Structures: Vibration Control through Boundary Conditioning Using Magnetorheological Elastomers, *Vibration*, Vol. 7, No. 2, pp. 605-626, 2024.

[16] W. C. Chi, X. G. Sun, Y. Q. Wang, Vibration control of piezoelectric beams with active constrained layer damping treatment using LADRC algorithm, in *Proceeding of*, Elsevier, pp. 106297.

[17] A. Gupta, S. Panda, R. S. Reddy, Damping capabilities of viscoelastic composites for active/passive constrained layer damping of the plate vibration: a comparative study, *Journal of Vibration Engineering & Technologies*, Vol. 12, No. 1, pp. 891-908, 2024.

[18] M. A. Kattimani, S. M. Hussain, P. Khasge, S. Mohrir, S. Suman, H. Masum, Utilizing finite element analysis to evaluate the monitoring of sandwich beam conditions, *Brazilian Journal of Development,* Vol. 10, No. 4, pp. e68942-e68942, 2024.

[19] I. Shardakov, A. Shestakov, I. Glot, G. Gusev, V. Epin, R. Tsvetkov, Piezoceramics Actuator with Attached Mass for Active Vibration Diagnostics of Reinforced Concrete Structures, *Sensors,* Vol. 24, No. 7, pp. 2181, 2024.

[20] H.-T. Liu, P.-H. Wang, W.-J. Wu, J.-Q. Li, 3D piezoelectric composite honeycombs with alternating bi-material beam: An active control method for elastic properties, *Materials Today Communications,* Vol. 38, pp. 108191, 2024.

[21] X. Yu, K. Huang, K. A. Alnowibet, Application of intelligent controller to speed up vibration attenuation of a sandwich smart structure subjected to external excitation, *Mechanics of Advanced Materials and Structures*, pp. 1-16, 2024.

[22] S. K. Shada, S. Kattimani, R. MR, Active layer damping of bi-directionally tapered functionally graded sandwich plates with 1-3 piezoelectric composites, *Mechanics of Advanced Materials and Structures*, pp. 1-20, 2024.

[23] Z. Guo, Optimized PI-PDF active structural acoustic control of smart FG GPL-reinforced closed-cell metallic foam sandwich plate, *Journal of Fluids and Structures,* Vol. 129, pp. 104168, 2024.

[24] Y. Zhang, Z. Wang, D. Tazeddinova, F. Ebrahimi, M. Habibi, H. Safarpour, Enhancing active vibration control performances in a smart rotary sandwich thick nanostructure conveying viscous fluid flow by a PD controller, *Waves in Random and Complex Media,* Vol. 34, No. 3, pp. 1835-1858, 2024.

[25] H. Luo, H. Li, X. Wu, G. Liu, W. Zhang, Dynamic Modeling and Active Vibration Control of Piezoelectric Laminated Structure Based on Macrofiber Composite, *Structural Control and Health Monitoring,* Vol. 2024, No. 1, pp. 8826434, 2024.

[26] X. G. Sun, W. C. Chi, Y. Q. Wang, Linear active disturbance rejection control algorithm for active vibration control of piezo-actuated beams: Theoretical and experimental studies, *Thin-Walled Structures,* Vol. 199, pp. 111782, 2024.

[27] Y. Zhang, W. Sun, H. Zhang, D. Du, K. Xu, H. Li, Vibration Analysis and Active Control of Irregular Integrated Composite Sandwich Plates with Incompletely Constrained Boundaries, *Available at SSRN 4803636*.

[28] R. Qi, L. Wang, X. Zhou, J. Xue, J. Jin, L. Yuan, Z. Shen, G. Deng, Embedded piezoelectric actuation method for enhanced solar wings vibration control, *International Journal of Mechanical Sciences,* Vol. 274, pp. 109271, 2024.

[29] A. Alsahlani, A. I. Alsabery, A. Al-Khateeb, A. A. Eidan, M. J. Alshukri, Vibration suppression of smart composite beam using model predictive controller, *Open Engineering,* Vol. 14, No. 1, pp. 20240001, 2024.

[30] Z. Xinyu, X. Yushan, W. Zhen, R. Xiaohui, HIGH PRECISION MODEL AND ACTIVE CONTROL FOR PIEZOELECTRIC INTELLIGENT FUNCTIONALLY GRADIENT SANDWICH STRUCTURES, *Chinese Journal of Theoretical and Applied Mechanics,* Vol. 56, No. 1, pp. 130-140, 2024.

[31] L. M. Essedik, T. Rachid, E. Madjid, C. Taha, C. Yasser, B. Mourad, R. Said, Active vibration control of piezoelectric multilayers FG-CNTRC and FG-GPLRC plates, *Polymer Composites*, 2024.

[32] F. Ebrahimi, M. F. Ahari, Active vibration control of the multilayered smart nanobeams: velocity feedback gain effects on the system's behavior, *Acta Mechanica,* Vol. 235, No. 1, pp. 493-510, 2024.

[33] Z. Wang, G. Cao, X. Meng, M. Rahimi, P. Rosaiah, M. R. Karim, A. Yvaz, S. Strashnov, Vibrational Analysis of Magneto-viscoelastic Bi-directional Functionally Graded Beams Subjected to Complex Environments Based on a Novel High-Order Shear Deformation Theory, *Journal of Vibration Engineering & Technologies,* Vol. 12, No. 4, pp. 5759-5770, 2024.

[34] M. Soltani, J. J. Fesharaki, S. A. Galehdari, R. T. Esfahani, M. Shahgholi, A comprehensive evaluation of the vibration control approach of the multi-layer sandwich composite piezoelectric micro-beam using higher-order elasticity theory and surface energy, in *Proceeding of*, Elsevier, pp. 105880.

[35] G. Han, Y. Wu, G. Hou, X. Xu, Investigation on parametric excitation vibration and piezoelectric active control of axially moving viscoelastic beams, *Journal of Vibration and Control*, pp. 10775463241260560, 2024.

[36] M. Jafari Niasar, A. A. Jafari, M. Irani Rahaghi, S. Mohammadrezazadeh, Active control of free and forced vibration of a rotating FG cylindrical shell via FG piezoelectric patches, *Mechanics Based Design of Structures and Machines*, Vol. 52, No. 7, pp. 3900-3924, 2024/07/02, 2024.

[37] T. Liu, C. Liu, Z. Zhang, Adaptive active vibration control for composite laminated plate: Theory and experiments, *Mechanical Systems and Signal Processing,* Vol. 206, pp. 110876, 2024.

[38] H. Pu, S. Fu, M. Wang, X. Fang, Y. Cai, J. Ding, Y. Sun, Y. Peng, S. Xie, J. Luo, Active vibration hybrid control strategy based on multi-DOFs piezoelectric platform, *Journal of Intelligent Material Systems and Structures*, Vol. 35, No. 3, pp. 352-366, 2024.

[39] Y. Wei, M. Al-Furjan, L. Shan, X. Shen, R. Kolahchi, M. Rabani bidgoli, A. Farrokhian, Micro-mass sensor-based vibration response of smart bidirectional functionally graded auxetic microbeams, *Archives of Civil and Mechanical Engineering*, Vol. 24, No. 1, pp. 38, 2024.

[40] C. Hameury, G. Ferrari, G. Franchini, M. Amabili, An experimental approach to multi-input multi-output nonlinear active vibration control of a clamped sandwich beam, *Mechanical Systems and Signal Processing*, Vol. 216, pp. 111496, 2024/07/01/, 2024.

[41] V. Rathi, A. A. Khan, Development of Vibration Annihilation of Sandwiched Beam with MROF DTSMC: A Novel Approach, 2024.

[42] M. Kim, Y.-B. Park, O. I. Okoli, C. Zhang, Processing, characterization, and modeling of carbon nanotube-reinforced multiscale composites, *Composites Science and Technology*, Vol. 69, No. 3-4, pp. 335-342, 2009.

[43] M. Safaei, P. Malekzadeh, M. R. Golbahar Haghighi, Out-of-plane moving load response and vibrational behavior of sandwich curved beams with GPLRC face sheets and porous core, *Composite Structures*, Vol. 327, pp. 117658, 2024/01/01/, 2024.

[44] F. Bargozini, M. Mohammadimehr, The theoretical and experimental buckling analysis of a nanocomposite beams reinforced by nanorods made of recycled materials, *Polymer Composites*, Vol. 45, No. 4, pp. 3327-3342, 2024.

[45] A. Ghorbanpour Arani, E. Haghparast, H. Babaakbar Zarei, Vibration of axially moving 3-phase CNTFPC plate resting on orthotropic foundation, *Structural Engineering and Mechanics*, Vol. 57, pp. 105-126, 01/10, 2016.

[46] M. Kolooli Mogehi, M. Mohammadimehr, N. Dình Duc, Vibration analysis of a sandwich Timoshenko beam reinforced by GOAM/CNT with various boundary conditions using VIM, *Materials Science and Engineering: B*, Vol. 304, pp. 117364, 2024/06/01/, 2024.

[47] V. N. Burlayenko, H. Altenbach, S. D. Dimitrova, Modal characteristics of functionally graded porous Timoshenko beams with variable cross-sections, *Composite Structures*, Vol. 342, pp. 118273, 2024/08/15/, 2024.

[48] P. Sourani, A. Ghorbanpour Arani, M. Hashemian, S. Niknejad, Nonlinear Dynamic Stability Analysis of Axially Moving CNTRC Piezoelectric Viscoelastic Nano/Micro Plate Based on MCST, *Journal of Computational Applied Mechanics*, Vol. 55, No. 2, pp. 242-274, 2024.

[49] M. Arefi, R. Karroubi, M. Irani-Rahaghi, Free vibration analysis of functionally graded laminated sandwich cylindrical shells integrated with piezoelectric layer, *Applied Mathematics and Mechanics*, Vol. 37, No. 7, pp. 821-834, 2016/07/01, 2016.

[50] N. Shahveisi, S. Feli, Dynamic and electrical responses of a curved sandwich beam with glass reinforced laminate layers and a pliable core in the presence of a piezoelectric layer under low-velocity impact, *Applied Mathematics and Mechanics*, Vol. 45, No. 1, pp. 155-178, 2024.

[51] Y. Akbari Birgani, A. Ghorbanpour Arani, Z. Khoddami Maraghi, Nonlocal buckling analysis of five-layer laminated nanocomposites on kerr foundation: A refined zigzag theory approach, *Journal of Sandwich Structures & Materials*, pp. 10996362241280020, 2024.

[52] N. A. Vu, T. D. Pham, T. T. Tran, Q.-H. Pham, Third-order isogeometric analysis for vibration characteristics of FGP plates in the thermal environment supported by Kerr foundation, *Case Studies in Thermal Engineering*, Vol. 45, pp. 102890, 2023/05/01/, 2023.

[53] B. R. Navi, M. Mohammadimehr, A. G. Arani, Active control of three-phase CNT/resin/fiber piezoelectric polymeric nanocomposite porous sandwich microbeam based on sinusoidal shear deformation theory, *Steel and Composite Structures*, Vol. 32, No. 6, pp. 753-767, 2019.

[54] H. S. Jouybary, A. M. Mabwe, D. A. Khaburi, A. El Hajjaji, An LMI-Based Linear Quadratic Regulator (LQR) Control for Modular Multilevel Converters (MMCs) Considering Parameters Uncertainty, *IEEE Access*, 2024.

[55] O. Saleem, J. Iqbal, Phase-Based Adaptive Fractional LQR for Inverted-Pendulum-Type Robots: Formulation and Verification, *IEEE Access*, 2024.

[56] A. Sachan, N. Kumar, SDN-enabled Quantized LQR for Smart Traffic Light Controller to Optimize Congestion, *ACM Trans. Internet Technol.*, Vol. 24, No. 1, pp. Article 7, 2024.

[57] B. Akgöz, Ö. Civalek, A size-dependent shear deformation beam model based on the strain gradient elasticity theory, *International Journal of Engineering Science,* Vol. 70, pp. 1-14, 2013/09/01/, 2013.

[58] P. R. Heyliger, F. Ramirez, E. Pan, Two-dimensional static fields in magnetoelectroelastic laminates, *Journal of Intelligent Material Systems and Structures,* Vol. 15, No. 9-10, pp. 689-709, 2004.

[59] K. Sharma, M. Shukla, Three-Phase Carbon Fiber Amine Functionalized Carbon Nanotubes Epoxy Composite: Processing, Characterisation, and Multiscale Modeling, *Journal of Nanomaterials,* Vol. 2014, No. 1, pp. 837492, 2014.

[60] F. H. Gojny, M. H. G. Wichmann, U. Köpke, B. Fiedler, K. Schulte, Carbon nanotube-reinforced epoxy-composites: enhanced stiffness and fracture toughness at low nanotube content, *Composites science and technology,* Vol. 64, No. 15, pp. 2363-2371, 2004.

[61] M. Li, C. Guedes Soares, R. Yan, Free vibration analysis of FGM plates on Winkler/Pasternak/Kerr foundation by using a simple quasi-3D HSDT, *Composite Structures,* Vol. 264, pp. 113643, 2021/05/15/, 2021.

Appendix A

To explain in more details how the interaction between the foundation parameters and the beam's material properties occur, and for obtaining $F_{elastic}$ in Eq. (39), it is assumed that the transverse displacement of the entire structure consists of two parts:

$$w(x,t) = w_1(x,t) + w_2(x,t) \tag{A-1}$$

where w_1 is transverse displacement of upper spring and w_2 is transverse deflection of lower elastic medium. The force generated between beam and upper spring is obtained as follows:

$$F_{elastic} = k_t w_1 \tag{A-2}$$

also, the government equation shear layer is written as follows:

$$F_{elastic} = k_b w_2 - k_G \frac{\partial^2 w_2}{\partial x^2} \tag{A-3}$$

in which k_t, k_b and k_G are top spring, bottom spring and shear layer constants, respectively. Substituting w_1 from Eq.(A-1) into Eq.(A-2) yields:

$$F_{elastic} = k_t(w - w_2) \tag{A-4}$$

then, Substituting w_2 from Eq.(A-4) into Eq.(A-3) yields the following equation:

$$F_{elastic} = k_b\left(w - \frac{F_{elastic}}{k_t}\right) - k_G \frac{\partial^2}{\partial x^2}\left(w - \frac{F_{elastic}}{k_t}\right) \tag{A-5}$$

After simplifying, one can obtain Eq. (39).